doi.org/10.52568/001506/JCSP/46.04.2024

A Type of Conjugated Fuse Heterocyclic Schiff Base Colorimetric and Fluorescent Chemosensors for Selective Detection of Picric acid (PA)

[1,2]Tianzhu Shi*, [2]Zhengfeng Xie, [1]Fuyong Wu, [1]Yulong Feng, [1]Tao Peng and [1]Dezhi Yuan*

[1]*Department of Brewing Engineering, Moutai Institute, Renhuai 564500, China.*

[2]*Oil & Gas Field Applied Chemistry Key Laboratory of Sichuan Province, College of Chemistry and Chemical Engineering, Southwest Petroleum University, Chengdu 610500, China.*

shitianzhu1018@163.com*

(Received on 10th March 2023, accepted in revised form 15th September 2023)

Summary: A series of Schiff base chemosensors (M1, M2 and M3) were designed and synthesized based on conjugated fuse heterocyclic aldehyde thiosemicarbazone. Optical properties of fluorescent probes M1, M2, and M3 toward various nitro explosives 2,4-dinitrotoluene (DNT), o-nitrophenol (ONP), p-nitrophenol (PNP), phenol (PhOH) and nitromethane (NM) were investigated, M1, M2, and M3 could selectively recognize PA with an obvious color change and fluorescence quenching, even in the presence of other coexistence nitro explosives. The detection limit of M1, M2, and M3 were 1.18×10^{-7} M, 1.13×10^{-7} M, 1.09×10^{-7} M, respectively.

Key Words: Schiff bases; Thiosemicarbazone; Fluorescence probe; Picric acid (PA).

Introduction

Highly explosive and explosive-like chemicals have a variety of applications in security operations and environmental protection, making the need for their sensitive and selective detection urgent [1-4]. Nitro compounds, including 2,4,6-trinitrotoluene (TNT), 2,4,6-trinitrophenol (TNP or Picric acid (PA)), and 2,4-dinitrophenol (DNP) are frequently employed as major components of several popular explosives. Additionally, PA is commonly utilized in the dye, explosives, pharmaceutical, leather, and leather industries [5-7]. It causes major health problems like cancer, anemia, liver malfunction, skin and eye irritation, and other conditions because of its higher water solubility and extensive use, which also pollutes groundwater and soil[8-11]. The selective, quick, and convenient detection of PA is therefore extremely important for reducing environmental contamination and locating buried explosives.

Several techniques for explosive materials, such as surface-enhanced Raman spectroscopy [12,13], Fourier-transform infrared [14], chromatography mass spectrometry[15-17], ion-mobility spectrometry [18-20], and electrochemical methods [21-23], which have been highly developed and employed. However, these techniques are confined to highly selective, quite expensive, time-consuming, and sophisticated instruments. Optically and fluorescence-based sensors, in contrast, have undergone substantial development because to their high sensitivity, rapid response, mobility, and simple sample preparation [24-26]. There is still a pressing need to investigate new fluorescent materials or reagents for the determination of PA, even though several fluorescence sensors (conjugated polymers (CPs) [27-29], Nanomaterials, Quantum dots (QDs) [30,31], Metal organic frameworks (MOFs) [32-34], gels [35], etc) have recently been developed for the rapid detection of nitro aromatics. PA is an anionic compound, which is typically identified by the development of a weak connection or chemical reaction between the subject and receptor molecules, in which hydrogen bonding plays a significant role. Intramolecular electron transfer and fluorescence amplification of the C=N double bond in the Schiff base skeleton were used to effectively detect PA [36,37].

Taking into account all of these factors and our prior research on Schiff base fluorescence sensors [38, 39], we have developed three organic small molecular based fluorescent sensors **M1**, **M2**, and **M3** (Table-1) by simple condensation reaction between aldehyde and thiosemicarbazide. We systematically investigated the respond of the three sensors to detecting traces of explosives including PA, 2,4-dinitrotoluene (DNT), o-nitrophenol (ONP), p-nitrophenol (PNP), phenol (PhOH) and nitromethane (NM) to evaluate the selectivity of the sensor. Fortunately, the three fluorescence sensors have good selectivity and high sensitivity toward PA.

*To whom all correspondence should be addressed.

Table-1: The list of nomenclature for abbreviations.

Abbreviation	Full name
M1	**(2E,2'E)-2,2'-(5,5'-(acenaphtho[1,2-b]quinoxaline-8,11-diyl)bis(thiophene-5,2-diyl))bis(methan-1-yl-1-ylidene)bis(hydrazinecarbothioamide)**
M2	**(2E,2'E)-2,2'-(5,5'-(acenaphtho[1,2-b]quinoxaline-8,11-diyl)bis(furan-5,2-diyl))bis(methan-1-yl-1-ylidene)bis(hydrazinecarbothioamide)**
M3	**(2E,2'E)-2,2'-(4,4'-(acenaphtho[1,2-b]quinoxaline-8,11-diyl)bis(4,1-phenylene))bis(methan-1-yl-1-ylidene)bis(hydrazinecarbothioamide)**

Experiment

Materials and Instrumentations

All of the chemicals and solvents were analytical-grade, and employed right away without any additional purification. To prepare initial solution (10^{-1} M), the mixture of several nitroaromatics was mixed in EtOH (3 mL) and then diluted to different concentration stocks for further usage. With a UV6000pc spectrophotometer, UV-Vis spectra were collected. A F-320 fluorescence spectrophotometer was used to obtain the fluorescence spectra. Melting points (m.p.) were measured without correction using an X-4 digital melting-point equipment. Tetramethylsilane served as an internal reference as the ^{1}H NMR and ^{13}C NMR spectra were collected at room temperature in DMSO-d_6 or $CDCl_3$ on a Varian Unity INOVA-400 NMR spectrometer. Using KBr pellets, IR spectra were collected using an EQUINOX 55 FT-IR spectrometer.

Synthesis of **M1-M3**

The synthesis of **M1**, **M2**, and **M3** were outlined in **Scheme 1**. 8,11-dibromoacenaphtho[1,2-b]quinoxaline **(3)** was synthesized and described by literature reported [40,41].

Synthesis of 5,5'-(acenaphtho[1,2-b]quinoxaline-8,11-diyl)dithiophene-2-carbaldehyde **(4)**:

The reaction mixture comprising 8,11-dibromoacenaphtho[1,2-b]quinoxaline (0.412 g, 1 mmol), 10 mL of 1.0 M K_2CO_3 aqueous solution, and a catalytic quantity of $Pd(PPh_3)_4$ (5 mol%) in 40 mL THF was heated to reflux for 0.5 h before the addition of 20 mL of (5-formylthiophen-2-yl) (0.780 g, 5 mmol). After cooling to ambient temperature, the mixture was refluxed for 12 h under N_2 environment. The orange precipitate was then filtered and washed three times with ethanol, water, and ethanol to produce orange precipitate in a 95% yield. FT-IR (cm^{-1}): 3088, 2809, 2785, 1647. ^{1}H NMR ($CDCl_3$, 400 MHz, ppm) δ 10.07 (s, 1H), 8.58 (d, *J* = 7.0 Hz, 1H), 8.25 (s, 1H), 8.20 (d, *J* = 8.3 Hz, 1H), 8.00 (d, *J* = 4.1 Hz, 1H), 7.97 – 7.90 (m, 1H), 7.88 (d, *J* = 4.1 Hz, 1H).

Synthesis of compounds **4-6:**

The reaction mixture comprising 8,11-dibromoacenaphtho[1,2-b]quinoxaline (0.412 g, 1 mmol), 10 mL of 1.0 M K_2CO_3 aqueous solution, and a catalytic quantity of $Pd(PPh_3)_4$ (5 mol%) in 40 mL THF was heated to reflux for 0.5 h and then injected 20 mL THF containing a certain boric acid aldehyde (5 mmol). After cooling to ambient temperature, the mixture was refluxed for 12 h under N_2 environment. The orange precipitate was then filtered and washed three times with ethanol, water and ethanol to give the precipitate in 80-90% yield. Compound **4**: Orange powder. FT-IR (cm^{-1}): 3088, 2809, 2785, 1647. ^{1}H NMR ($CDCl_3$, 400 MHz, ppm) δ 10.07 (s, 1H), 8.58 (d, *J* = 7.0 Hz, 1H), 8.25 (s, 1H), 8.20 (d, *J* = 8.3 Hz, 1H), 8.00 (d, *J* = 4.1 Hz, 1H), 7.97 – 7.90 (m, 1H), 7.88 (d, *J* = 4.1 Hz, 1H).

Compound **5**: Orange powder. FT-IR(cm^{-1}): 3050, 2796, 2690, 2676. 1676. ^{1}H NMR ($CDCl_3$, 400 MHz, ppm) δ 9.80 (s, 1H), 8.51 (s, 1H), 8.46 (d, *J* = 7.0 Hz, 1H), 8.28 (d, *J* = 3.7 Hz, 1H), 8.19 (d, *J* = 8.2 Hz, 1H), 7.90 (dd, *J* = 8.2, 7.0 Hz, 1H), 7.50 (d, *J* = 3.7 Hz, 1H).

Compound **6**: Yellow powder. FT-IR (cm^{-1}): 3030, 2809, 2715, 1695. ^{1}H NMR (400 MHz, $CDCl_3$, ppm) δ 10.19 (s, 1H), 8.32 (d, *J* = 6.9 Hz, 1H), 8.12 (dd, *J* = 8.3, 4.9 Hz, 3H), 8.07 (d, *J* = 8.3 Hz, 2H), 7.93 (s, 1H), 7.87 – 7.78 (m, 1H).

Synthesis of **M1 - M3**:

A mixture of compound 4, 5, or 6 (0.5 mmol) and thiosemicarbazide (0.25 mmol) was added to 25 mL flask followed by 0.5 mL glacial acetic acid in 10 mL absolute ethanol. The mixture was refluxed for 7 h to obtain the precipitate, which was filtered and dried under vacuum to obtain the pure compound in 80-90% yield.

M1: Red solid powder, m.p. >300 ℃. FT-IR (cm^{-1}): 3418, 3261, 3154, 1584, 1535, 1292. ^{1}H NMR (400 MHz, DMSO, ppm) δ 11.57 (s, 1H), 8.58 (d, *J* = 7.0 Hz, 1H), 8.44 – 8.30 (m, 4H), 8.13 (d, *J* = 4.1 Hz, 1H), 8.06 – 7.96 (m, 1H), 7.80 (s, 1H), 7.60 (d, *J* = 4.1 Hz, 1H). ^{13}C NMR (100 MHz, DMSO, ppm) δ 177.69, 152.15, 141.73, 140.40, 138.09, 136.85, 136.29, 131.31, 130.76, 130.54, 130.24, 129.85, 129.32, 128.20, 127.05, 123.31. HR-MS (TOF-MS): m/z = 621.0847 ($[M+H]^+$), 419.2335 ($[M+H-2C_2H_3N_3S]^+$), calcd for $(C_{30}H_{20}N_8S_4)^+$ = 621.0772.

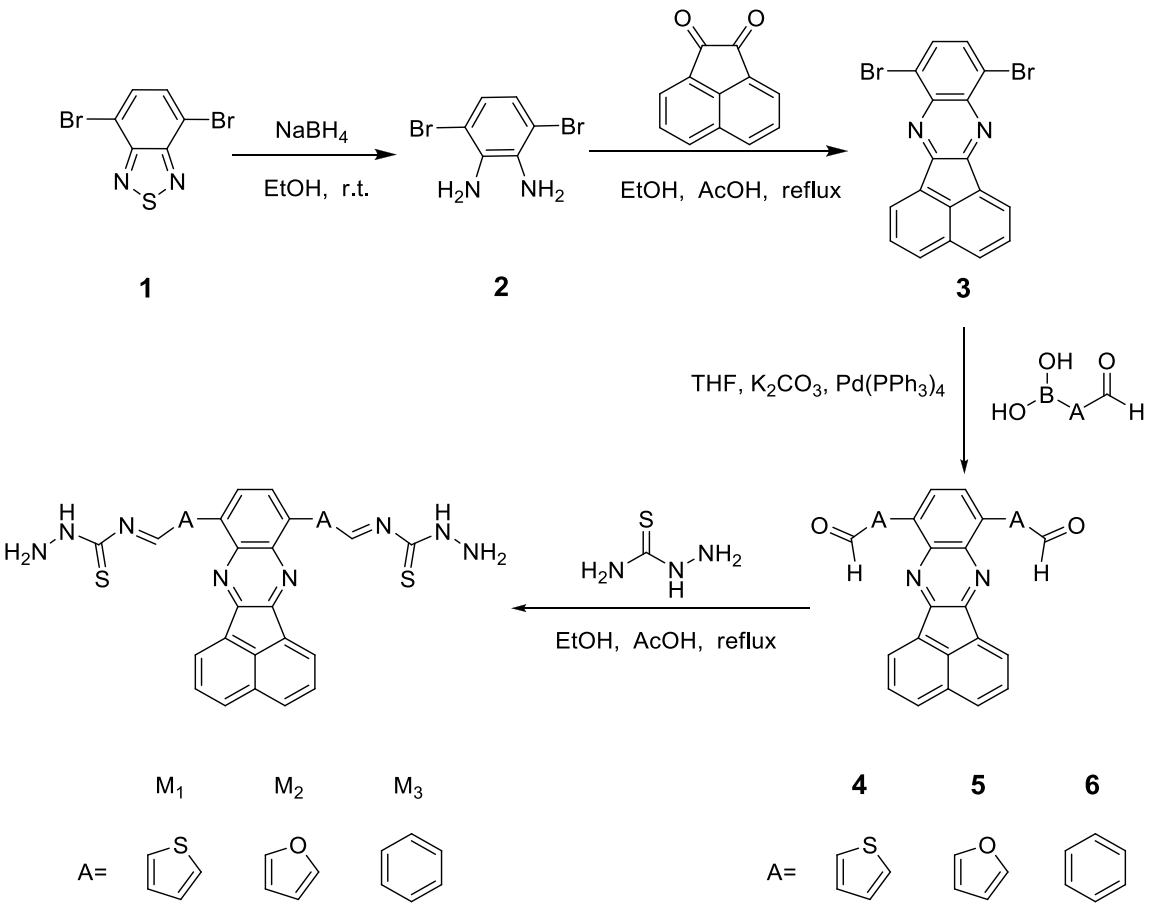

Scheme-1: Synthesis of **M1 - M3**.

M2: Red solid powder, m.p. >300 ℃. FT-IR (cm^{-1}): 3418, 3254, 3149, 1576, 1524, 1274. ^{1}H NMR (400 MHz, DMSO, ppm) δ 11.60 (s, 1H), 8.50 (d, *J* = 7.0 Hz, 1H), 8.37 (s, 2H), 8.29 (d, *J* = 8.2 Hz, 1H), 8.15 (d, *J* = 3.6 Hz, 1H), 8.08 (s, 1H), 7.98 – 7.89 (m, 1H), 7.82 (s, 1H), 7.22 (d, *J* = 3.6 Hz, 1H). ^{13}C NMR (100 MHz, DMSO, ppm) δ 177.91, 152.49, 151.53, 149.15, 136.86, 136.10, 132.00, 130.87, 130.37, 129.79, 129.17, 126.82, 125.69, 122.73, 116.72, 116.25. HR-MS (TOF-MS): m/z = 589.1200, calcd for $(C_{30}H_{21}N_8O_2S_2)^+$ = 589.1229 ($[M+H]^+$).

M3: Faint yellow solid powder, m.p. >300 ℃. FT-IR (cm^{-1}): 3379, 3254, 3152, 1586, 1528, 1281. ^{1}H NMR (400 MHz, DMSO) δ 11.52 (s, 1H), 8.27 (dd, *J* = 11.5, 7.7 Hz, 3H), 8.21 (s, 1H), 8.07 (s, 1H), 8.04 – 7.96 (m, 3H), 7.90 (dd, *J* = 7.7, 6.0 Hz, 3H). ^{13}C NMR (101 MHz, DMSO) δ 178.16, 152.78, 142.20, 139.98, 139.65, 138.68, 136.13, 133.65, 131.42, 131.27, 130.26, 130.02, 129.95, 129.32, 127.12, 122.36. HR-MS (TOF-MS): m/z = 609.1622, calcd for $(C_{34}H_{25}N_8S_2)^+$ = 609.1643 ($[M+H]^+$).

Results and Discussion

The optical properties of each compound **M1**, **M2** and **M3** were studied with the help of UV−Vis absorption and fluorescence spectroscopy. As we can see from **Fig. S1**, the solution of **M1** and **M2** exhibited only a little absorbance at 377 nm and 372 nm in UV-Vis spectrum, upon excitation at 377 and 372 nm, they showed strong fluorescence intensity with emission maxima at 634 nm and 628nm. And a similar situation can be observed for **M3** at 330 nm in UV-Vis spectrum and at 520 nm in fluorescence spectrum. To ascertain the ability of the as-synthesized fluorescent sensors **M1**, **M2** and **M3** in sensing trace amounts of nitro explosives, the optical response experiments were carried out in DMSO/H_2O (4:1 *v*/*v*) by adding 10 equiv. of various nitro explosives such as picric acid (PA), 2,4-dinitrophenol (2,4-DNP), *o*-nitrophenol (ONP), *p*-nitrophenol (PNP), phenol (PhOH), Nitromethane

(NM). Among these nitro explosives, quite large fluorescence quenching were observed after 10 equiv. of PA added immediately. Whereas, except DNP quenched half, other nitro explosives had minor effects on the fluorescence intensity of **M1**, **M2** and **M3** (Fig. 1a). This probably because the structure of DNP and PA are similar and have the similar chemical properties. The quenching efficiency for these sensors achieved to 95% for **M1**, 91% for **M2** and 94% for **M3.** In addition to this, upon addition of PA to the solution of **M1**, **M2** and **M3**, the distinct fluorescence change can be observed by visual inspection under normal light and UV light irradiation as shown in Fig. 1b.

For the purpose of further investigate the selective sensing of PA, the fluorescence quenching titration experiments with PA were performed. As shown in Fig. 2, the incremental addition of PA (0 to 10 equiv.) to the solution of **M1**, **M2** and **M3** all resulted in gradual fluorescence quenching in fluorescence spectra and steady absorbance increasing in UV-Vis spectra. The **Fig. S2** showed the correlation of **M1**, **M2** and **M3** with PA. From **Fig. S2**, it can be seen that **M1**, **M2** and **M3** show a good linear relationship at lower concentrations but a close exponent correlation at higher concentrations. And the detection limit were calculated as 1.18×10^{-7} M, 1.13×10^{-7} M, 1.09×10^{-7} M respectively (3σ) [42].

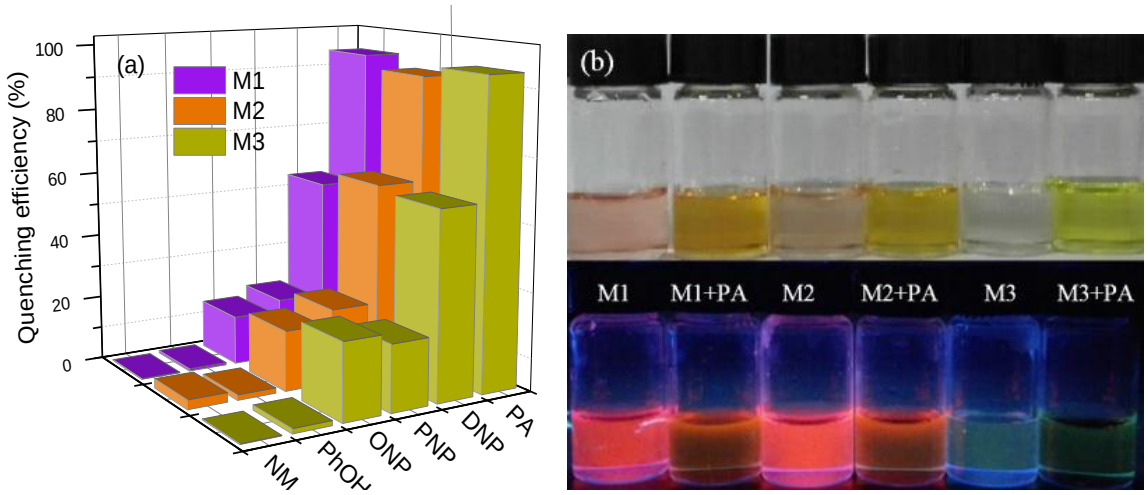

Fig. 1: (a) Quenching efficiency of **M1**, **M2**, **M3** toward different nitro aromatic compounds and (b) Fluorescence color change of the solution of **M1**, **M2** , **M3** and **M1**, **M2** , **M3** induced by PA under a portable UV lamp in DMSO/H_2O (4:1 *v/v*).

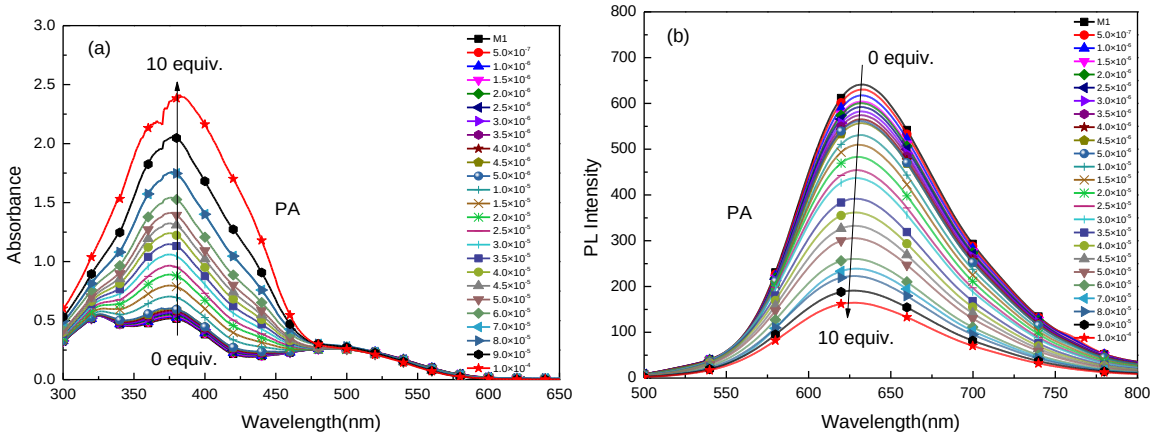

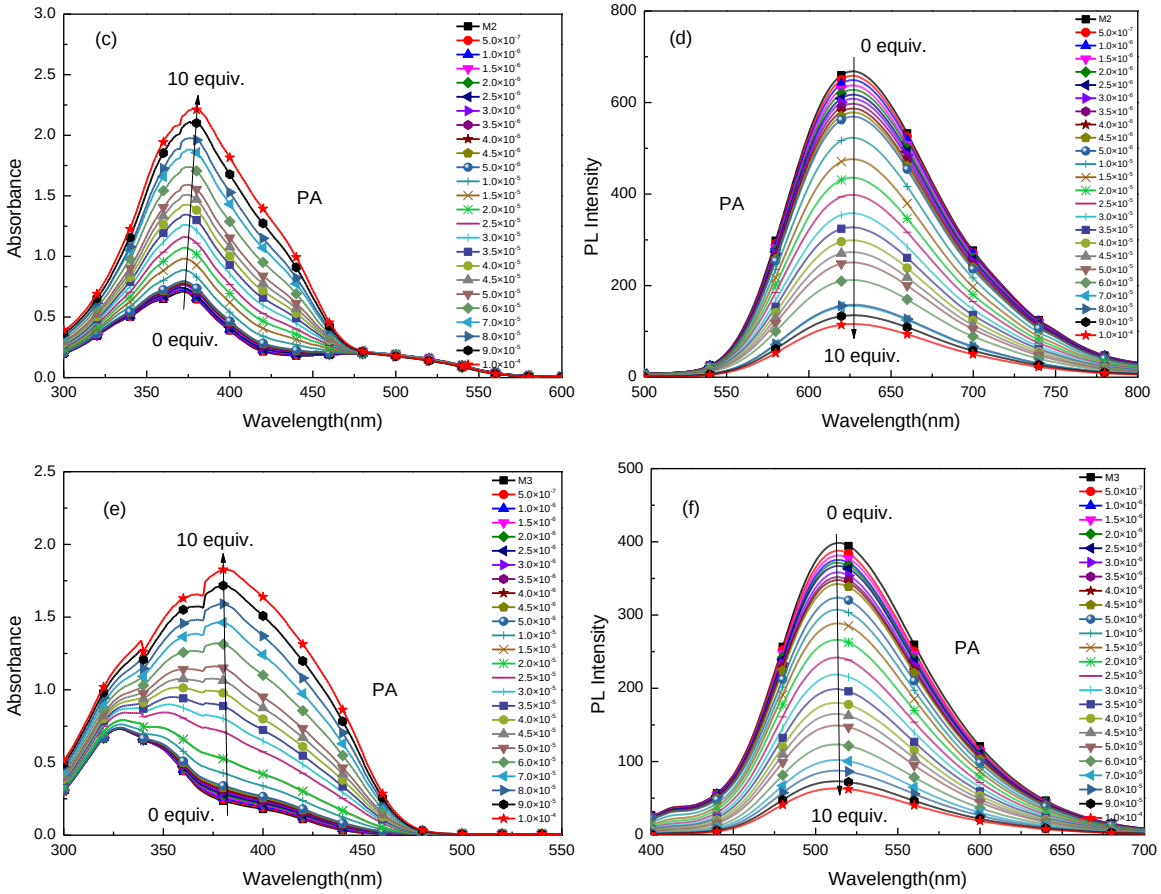

Fig. 2: (a) Absorbance spectra and (b) Fluorescence spectra of PA titration with M1 in 4:1 DMSO/H_2O; (c) Absorbance spectra and (d) Fluorescence spectra of PA titration with M2 in 4:1 DMSO/H_2O; (e) Absorbance spectra and (f) Fluorescence spectra of PA titration with M3 in 4:1 DMSO/H_2O.

To get an insight into the mechanism of PA detection, we have also performed fluorescence quenching titration experiment with all other nitro explosives. For these nitro explosives, different degrees of fluorescence quenching have also been observed (Fig. 3). In comparison to the linear increasing responses registered for all other nitro explosives, an upward bending can be seen only in case of consecutive addition of PA toward the solution of **M1**, **M2** and **M3**. Furthermore, the quenching efficiency for all the nitro explosives were analyzed using Stern−Volmer (SV) equation and the K_{SV} values of **M1**, **M2** and **M3** for PA are 3.35×10^4 M^{-1}, 3.51×10^4 M^{-1} and 3.63×10^4 M^{-1}, which larger than those for other nitro explosives. These large K_{SV} values indicate that the as-prepared fluorescent sensors are very predominant selective and sensitive to PA from other nitro explosives. We also carried out nuclear magnetic titration experiment to study the mechanism of PA detection by taking M1 as an example. As shown in Fig. 4, when DMSO-d_6 solution of 2.0 equiv. PA was added to DMSO- d_6 solution of M1, the N-H peak at δ11.56 ppm did not move, indicating that the N-H part of thiosemarbazone did not participate in the recognition of PA. The peak of NH_2 at δ 8.34 ppm moved to 8.27 ppm, and the peak of NH_2 at δ 7.71 ppm gradually disappeared, indicating that NH_2 in thiosemicarbazone participated in PA recognition. Moreover, when PA solution of 3.0 equiv. was added, the spectra did not change, indicating that M1 and PA were combined in a 1:2 molar ratio. Accordingly, we conclude that the possible recognition mechanism of PA by M1, M2 and M3 is shown in Fig. 5. On the other hand, such remarkable selectivity and the exceptional quenching efficiency by PA can be explained via the photoinduced electron transfer (PET) quenching process because of their inherently high electron affinity [43, 44].

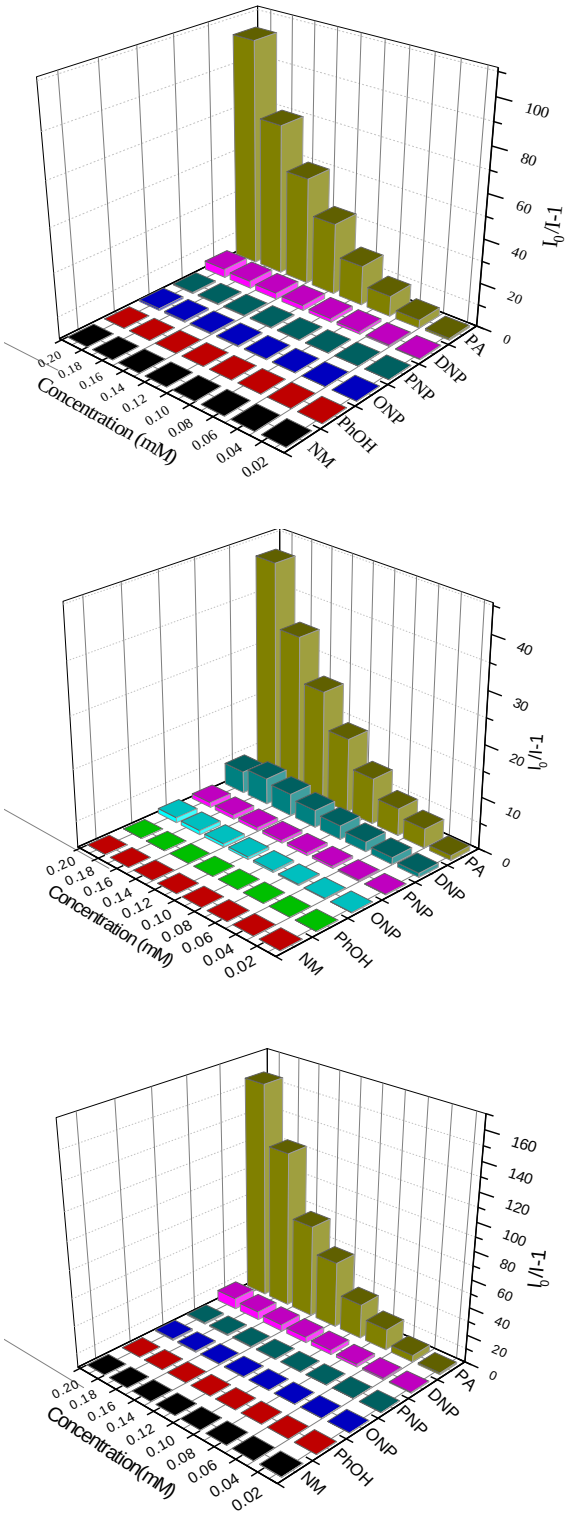

Fig. 3: Stern − Volmer plot of **M1**, **M2** and **M3** for all nitro compounds.

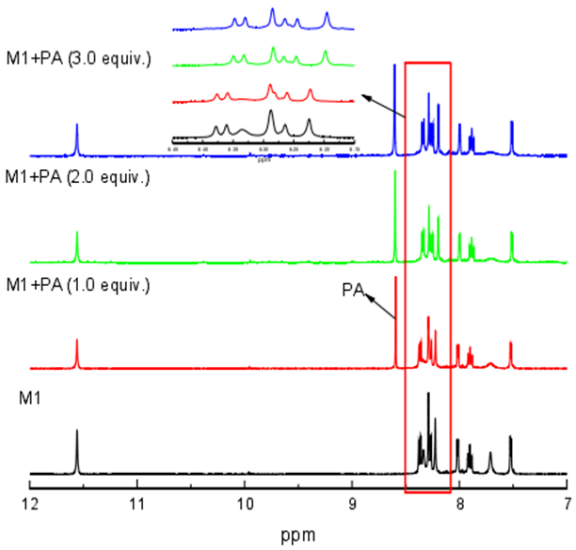

Fig. 4: ^{1}H NMR spectra of M1+PA nuclear magnetic titration experiment.

Following a planned investigational protocol, competition experiments in the presence of other nitro explosives were examined. The solution of **M1**, **M2** and **M3** were initially treated with 10 equiv. of NM to access most of the binding sites of the composite followed by 10 equiv. of PA and the same process is carried-out for other nitro aromatics. Much intriguingly, subsequent PA addition resulted in a strikingly prompt and noteworthy PL-quenching response, and similar kinds of results were also noticed for the DNP experiments (Fig. 6). These results further confirmed very excellent selectivity of **M1**, **M2** and **M3** toward PA.

Conclusion

In conclusion, we have created the **M1**, **M2**, and **M3** conjugated fuse heterocyclic aldehyde thiosemicarbazone Schiff bases. All of the compounds had extremely high binding affinities for PA, according to a fluorescence titration analysis. The quenching of the fluorescence was caused by resonance energy transfer between the PA and the sensors. Consequently, **M1**, **M2**, and **M3** may be used as a selective and reversible PA optical indicator.

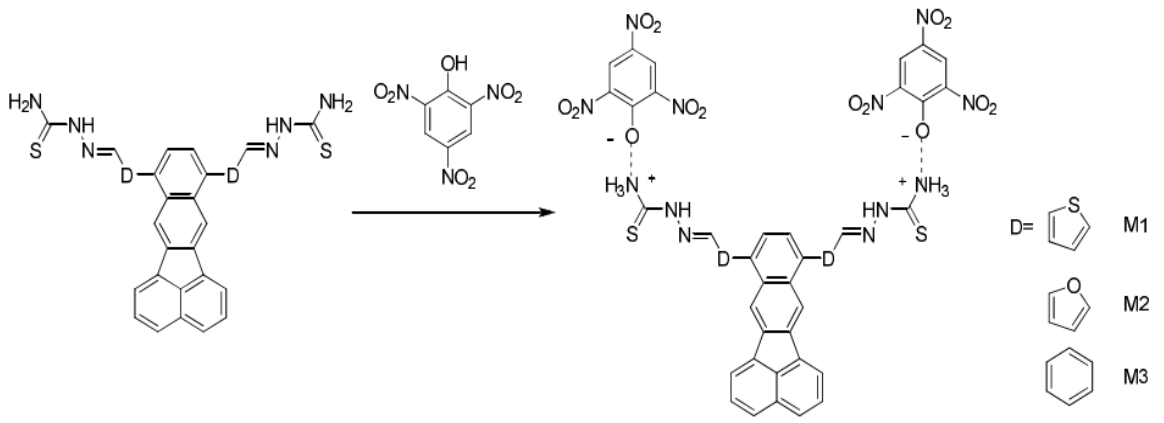

Fig. 5: The proposed mechanism of M1, M2, M3 toward PA.

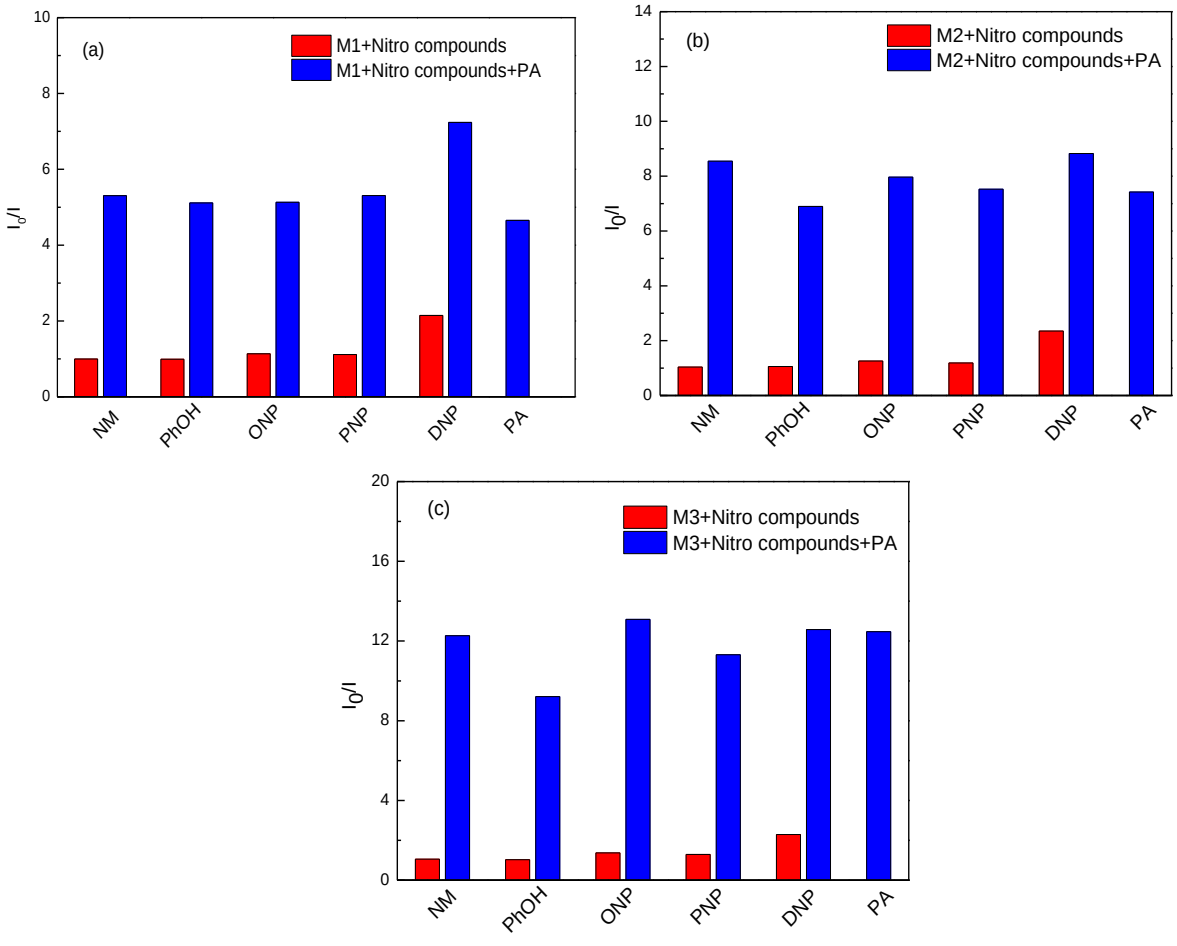

Fig. 6: Fluorescence quenching response of (a) **M1**, (b) **M2** and (c) **M3** upon addition of various nitro-explosive analytes followed by PA.

Acknowledgement

We are grateful for the financial support from the Fund of Zunyi Technology and Big data Bureau, Moutai institute Joint Science and Technology Research and Development Project (ZSKHHZ [2021] No. 333, ZSKHHZ [2020] No.313, ZSKHHZ [2021] No.322, ZSKHHZ [2021] No.313), Zunyi Outstanding Youth Science and technology innovation talents training project (ZunYouQingKe [2021] 7), the Fund of the young scientific and technological talents growth project of Guizhou Provincial Department of Education (QianJiaoHe KY Zi [2020] 238), Research Foundation for Scientific Scholars of Moutai Institute (Grant No. mygccrc[2022]007, mygccrc [2022] 022, mygccrc [2022] 014, mygccrc [2022]094).

Reference

1. M. E. Germain, M. J. Knapp, Optical explosives detection: from color changes to fluorescence turn-on. *Chem. Soc. Rev.*, **38**, 2543 (2009).
2. Y. Ma, S. Wang, L. Wang, Nanomaterials for luminescence detection of nitroaromatic explosives. *TrAC Trends in Analytical Chemistry*, **65**, 13 (2015).
3. A. Chowdhury, P.S. Mukherjee, Electron-Rich Triphenylamine-Based Sensors for Picric Acid Detection. *J. Org. Chem.*, **80**, 4064 (2015).
4. X. Sun, Y. Liu, G. Shaw, et al. Fundamental study of electrospun pyrene–polyethersulfone nanofibers using mixed solvents for sensitive and selective explosives detection in aqueous solution. *ACS Appl. Mater. Interfaces* **7**, 13189 (2015).
5. B. Gogoi, N. Sen Sarma, Curcumin-Cysteine and Curcumin-Tryptophan Conjugate as Fluorescence Turn On Sensors for Picric Acid in Aqueous Media. *ACS Appl. Mater. Interfaces*, **7**, 11195, (2015) .
6. S. Mukherjee, A.V. Desai, A.I Inamdar, et al. Selective Detection of 2, 4, 6-Trinitrophenol (TNP) by a π-Stacked Organic Crystalline Solid in Water. *Cryst. Growth Des.* **15**, 3493 (2015).
7. V. Bhalla, S. Kaur, V. Vij, M. Kumar, Mercury-Modulated Supramolecular Assembly of a Hexaphenylbenzene Derivative for Selective Detection of Picric Acid. *Inorg. Chem.*, **52**, 4860 (2013).
8. J. Wyman, M. Serve, D. Hobson, et al Safety data sheet for picric acid, resource of National Institute of Health. *J. Toxicol. Environ. Health, Part A* , **37**, 313 (1992).
9. M. Kumar, S.I Reja, V. Bhalla, A charge transfer amplified fluorescent Hg^{2+} complex for detection of picric acid and construction of logic functions. *Org. Lett.*, **14**, 6084 (2012).
10. J. Shen, J. Zhang, Y. Zuo, et al. Biodegradation of 2, 4, 6-trinitrophenol by Rhodococcus sp. isolated from a picric acid-contaminated soil. *J. Hazard. Mater.*, **163**, 1199 (2009).
11. T.P. Huynh, M. Sosnowska, J.W. Sobczak, et al. Simultaneous chronoamperometry and piezoelectric microgravimetry determination of nitroaromatic explosives using molecularly imprinted thiophene polymers. *Anal. Chem.*, **85**, 8361 (2013).
12. J.M. Sylvia, J.A. Janni, J. Klein, Surface-enhanced Raman detection of 2, 4-dinitrotoluene impurity vapor as a marker to locate landmines. *Anal. Chem.*, **72**, 5834 (2000).
13. S.S. Dasary, A.K. Singh, D. Senapati, et al. Gold nanoparticle based label-free SERS probe for ultrasensitive and selective detection of trinitrotoluene. *J. Am. Chem. Soc.*, **131**, 13806 (2009).
14. M. López-López, C. García-Ruiz, Infrared and Raman spectroscopy techniques applied to identification of explosives. *TrAC Trends in Anal. Chem.*, **54**, 36 (2014).
15. J.I. Steinfeld, J. Wormhoudt, Explosives detection: a challenge for physical chemistry. *Annu. Rev. Phys. Chem.*, **49**, 203 (1998).
16. N. Talaty, C.C. Mulligan, D.R. Justes, et al. Fabric analysis by ambient mass spectrometry for explosives and drugs. *Analyst*, **133**, 1532 (2008).
17. L. Barron, E. Gilchrist, Ion chromatography-mass spectrometry: A review of recent technologies and applications in forensic and environmental explosives analysis. *Anal. Chim. Acta*, **806**, 27 (2014).
18. M. Tam, H.H. Hill, Secondary electrospray ionization-ion mobility spectrometry for explosive vapor detection. *Anal. Chem*, **76**, 2741 (2004).
19. M. Najarro, M.E.D. Morris, M.E. Staymates, et al. Optimized thermal desorption for improved sensitivity in trace explosives detection by ion mobility spectrometry. *Analyst*, **137**, 2614 (**2012**).
20. K.M. Roscioli, E. Davis, W.F. Siems, et al. Modular ion mobility spectrometer for explosives detection using corona ionization. *Anal. Chem.*, **83**, 5965 (2011).
21. E.S. Forzani, D Lu, M.J Leright, et al. A hybrid electrochemical−colorimetric sensing platform for detection of explosives. *J. Am. Chem. Soc.*,

131, 1390 (2009).
22. J. Yang, T.M. Swager, Fluorescent porous polymer films as TNT chemosensors: electronic and structural effects. *J. Am. Chem. Soc.*, **120**, 11864 (1998).
23. R. Zhang, C. Sun, Y. Lu, Graphene Nanoribbon-Supported PtPd Concave Nanocubes for Electrochemical Detection of TNT with High Sensitivity and Selectivity. *Anal. Chem.*, **87**, 12262 (2015).
24. J. Xiong, J. Li, G. Mo, et al. Benzimidazole derivatives: selective fluorescent chemosensors for the picogram detection of picric acid. *J. Org. Chem.*, **79**, 11619 (2014).
25. M. Rong, L. Lin, X. Song, et al. A Label-Free Fluorescence Sensing Approach for Selective and Sensitive Detection of 2, 4, 6-Trinitrophenol (TNP) in Aqueous Solution Using Graphitic Carbon Nitride Nanosheets. *Anal. Chem.*, **87**, 1288 (2014).
26. B. Roy, A.K. Bar, B. Gole, Fluorescent tris-imidazolium sensors for picric acid explosive. *J. Org. Chem.*, **78**, 1306 (2013).
27. A.H. Malik, S. Hussain, A. Kalita, Conjugated polymer nanoparticles for the amplified detection of nitro-explosive picric acid on multiple platforms. *ACS Appl. Mater. Interfaces*, **7**, 26968 (2015)
28. P.G. Del Rosso, M.J. Romagnoli, M.F. Almassio, et al. Diphenylanthrylene and diphenylfluorene-based segmented conjugated polymer films as fluorescent chemosensors for nitroaromatics in aqueous solution. *Sensors and Actuators B: Chemical*, **203**, 612 (2014).
29. S.J. Toal, W.C. Trogler, Polymer sensors for nitroaromatic explosives detection. *J. Mater. Chem.*, **16**, 2871 (2006).
30. L. Lin M. Rong, S. Lu, et al. A facile synthesis of highly luminescent nitrogen-doped graphene quantum dots for the detection of 2, 4, 6-trinitrophenol in aqueous solution. *Nanoscale*, **7**, 1872 (2015).
31. S. Xu, H. Lu, J. Li, et al. Dummy molecularly imprinted polymers-capped CdTe quantum dots for the fluorescent sensing of 2, 4, 6-Trinitrotoluene. *ACS Appl. Mater. Interfaces*, **5**, 8146 (2013).
32. Z. Hu, B.J. Deibert J. Li, Luminescent metal–organic frameworks for chemical sensing and explosive detection. *Chem. Soc. Rev.*, **43**, 5815 (2014).
33. S.S. Nagarkar, A.V. Desai, S.K. Ghosh, A fluorescent metal–organic framework for highly selective detection of nitro explosives in the aqueous phase. *Chem. Commun.*, **50**, 8915 (2014).
34. S. Sanda, S. Parshamoni, S. Biswas, Highly selective detection of palladium and picric acid by a luminescent MOF: a dual functional fluorescent sensor. *Chem. Commun.*, **51**, 6576 (2015).
35. N. Dey, S.K. Samanta, S. Bhattacharya, Selective and efficient detection of nitro-aromatic explosives in multiple media including water, micelles, organogel, and solid support. *ACS Appl. Mater. Interfaces*, **5**, 8394 (2013).
36. J.M. Delente, D. Umadevi, Shanmugaraju, S. et al. Aggregation induced emission (AIE) active 4-amino-1,8-naphthalimide-Troger's base for the selective sensing of chemical explosives in competitive aqueous media. *Chem Commun (Camb),*, **56**, 2562 (2020).
37. M.E.H. Fassbender, Y. Huang, Y. Hu, et al. Selective biosorption of thorium (IV) from aqueous solutions by ginkgo leaf. *Plos One*, **13**, e0193659 (2018).
38. Y. Chen, W. Shi, Y. Hui, et al. A new highly selective fluorescent turn-on chemosensor for cyanide anion. *Talanta*, **137**, 38 (2015).
39. H. Lin, W. Shi, Y. Tian, et al. A simple and highly selective 'turn-on'type fluorescence chemodosimeter for Hg^{2+} based on 1-(2-phenyl-2*H*-[1,2,3]triazole-4-carbonyl) thiosemicarbazide. *J. Lumin.*, **157**, 280 (2015).
40. D. Hong, R. Lee, R.G. Choi, et al. Self-organized spiral columns in laterally grafted rods. *Chem. Commun*., **46**, 4896 (2010).
41. Z. Guo, T. Lei, Z. Jin, et al.T-Shaped Donor-Acceptor Molecules for Low-Loss Red-Emission Optical Waveguide. *Org. Lett.*, **15**, 3530 (2013).
42. V. Thomsen, D. Schatzlein, D. Mercuro, Limits of detection in spectroscopy. *Spectroscopy*, **18**, 112 (2003).
43. B. Xu, X. Wu, H. Li, et al. Selective detection of TNT and picric acid by conjugated polymer film sensors with donor–acceptor architecture. *Macromolecules*, **44**, 5089 (2011).
44. M. Bai, S. Huang, S. Xu, et al. Fluorescent Nanosensors via Photoinduced Polymerization of Hydrophobic Inorganic Quantum Dots for the Sensitive and Selective Detection of Nitroaromatics. *Anal. Chem.*, **87**, 2383 (2015).